The Journal of Neuroscience, May 1993, 13(5): 1976–1992

Na^+ Channel Immunolocalization in Peripheral Mammalian Axons and Changes following Nerve Injury and Neuroma Formation

Marshall Devor,[1] Ruth Govrin-Lippmann,[1] and Kimon Angelides[2]

[1]Department of Cell and Animal Biology, Life Sciences Institute, Hebrew University of Jerusalem, Jerusalem 91904, Israel and [2]Department of Cell Biology, Baylor College of Medicine, Houston, Texas 77030

Nerve injury frequently triggers hyperexcitability and the ectopic initiation of impulses in primary afferent axons. An important consequence is neuropathic paresthesias and pain. Electrogenesis in *normal* afferents depends on appropriate Na^+ channel concentrations. Therefore, we have asked whether injury might trigger changes in axolemmal Na^+ channel distribution that could account for neuropathic hyperexcitability. We used an Na^+ channel-specific antibody, 7493, to immunolocalize Na^+ channels ultrastructurally in membranes of normal rat axons, and to assess remodeling following nerve section and neuroma formation. Selective labeling of nodal axolemma and, more weakly, of Schwann cell membrane, confirmed the efficacy of our immunolabeling protocol. In neuromas at postoperative times associated with peak ectopic activity, we found clear evidence of Na^+ channel accumulation. Specifically, soon after myelin was stripped from large-diameter axons, the exposed, formerly internodal axolemma became immunopositive. Small-diameter unmyelinated axons and axon sprouts in the neuroma were also marked with 7493 IgG. Activated phagocytic macrophages and endothelial cells were 7493 negative. Both large- and small-diameter axons in neuromas end in swollen, organelle-packed "end bulbs." Most, but not all, of these acquired Na^+ channel immunolabeling. We propose that remodeling results from a modification of the normal process of Na^+ channel turnover in neural membranes. Na^+ channel protein accumulates in preterminal axolemma and neuroma end bulbs due to a combination of permissive factors (especially myelin removal) and promotional factors (removal of normal downstream targets). This accumulation is a likely precursor of afferent hyperexcitability in injured nerve.

[Key words: ectopic hyperexcitability, membrane remodeling, nerve injury, neuroma, pain, sodium channels]

The ability of neurons to initiate trains of action potentials depends on the presence of transmembrane proteins that serve as regulated channels for ionic current flow. A uniquely important one in this process is the voltage-sensitive Na^+ channel (Hille, 1984). Most vertebrate neurons have a localized, Na^+ channel–rich membrane patch that serves to encode integrated depolarizations from dendritic and somatic inputs into an appropriate firing pattern. Usually this encoding region lies near the cell soma: the axon hillock or the first node of Ranvier (Dodge and Cooley, 1973; Waxman and Quick, 1978; Matsumoto and Rosenbluth, 1985; Wollner and Catterall, 1986). An exception is the primary afferent neuron, in which this zone is displaced to the far distal end of the peripheral axon, often centimeters or even meters from the cell soma. Here it serves as a sensory transducer ending.

The sensory end of afferent axons is highly specialized for translating stimulus-evoked depolarizations (generator potential) into spike trains. This capability is absent over the rest of the axon. For example, mechanical or thermal stimulation in mid-nerve, or even direct injection of depolarizing current through an intracellular microelectrode, does not yield sustained firing (Ruiz et al., 1981).

In contrast to the midnerve part of intact axons, many chronically injured afferents are able to sustain repetitive discharge. This ectopic rhythmic firing capability develops with time at formerly mid-nerve sites, yielding foci of abnormal evoked and spontaneous afferent discharge (Koschorke et al., 1991; Devor, 1993). In recent years a good deal of evidence has accumulated establishing activity originating at such ectopic neural pacemaker sites as an important cause of neuropathic paresthesias and pain in nerve injured patients (Nystrom and Hagbarth, 1981; Ochoa et al., 1982; Nordin et al., 1984; Devor, 1993).

These indications of a causal link between abnormal neural activity and neuropathic pain motivate a search for the cellular mechanism responsible for the development of ectopic firing capability in afferents. Since impulse initiation at *normal* locations is dependent on Na^+ channels, we have used an Na^+ channel–specific antibody to look for possible changes in Na^+ channel distribution at sites of nerve injury associated with ectopic firing.

Materials and Methods

Subjects and surgery. We used adult (>300 gm) male Wistar-derived Sabra strain rats. Work followed ethical guidelines of the International Association for the Study of Pain (IASP), and university and national regulations on humane use of research animals. Under Nembutal anesthesia (50 mg/kg, i.p.), the sciatic nerve was exposed in the popliteal fossa and tightly ligated with 5-0 silk. The nerve was then cut across about 1 mm distal to the ligature, and about 5 mm of the distal stump was excised. Alternatively, the L4 and L5 dorsal roots (DRs) were exposed in a lumbar laminectomy, tightly ligated with 6-0 silk ≈3–5 mm from their point of entry into the spinal cord, and cut between the ligature and the cord. In some rats both lesions were carried out. Incisions were closed in layers, and topical and systemic antibiotics administered. Recovery was uneventful. This nerve/DR injury, designed

Received Mar. 9, 1992; revised Nov. 6, 1992; accepted Nov. 11, 1992.

We acknowledge the helpful comments of S. G. Waxman, J. A. Black, and M. H. Ellisman. This work was supported by grants from the United States–Israel Binational Science Foundation (BSF), the Hebrew University Center for Research on Pain, the (U.S.) National Multiple Sclerosis Society, and the U.S. National Institutes of Health (NIH Grant CNS28072).

Correspondence should be addressed to Prof. Marshall Devor at the above address.

to suppress regeneration and promote neuroma formation, is identical to that used in our prior electrophysiological and anatomical studies of experimental neuromas (reviewed in Devor, 1993).

The rats were maintained postoperatively under standard colony conditions. At appropriate times they were deeply anesthetized and perfused transcardially with saline followed by 4% paraformaldehyde in 0.1 M PO_4 buffer (37°C, pH 7.4). After ≈30 min postfixation *in situ*, tissue was removed and postfixed for an additional 2–3 hr at 4°C. In addition to neuromas and proximal nerve and DR segments, control samples of intact contralateral nerves and DRs were also taken.

Immunostaining. The results are based primarily on DR and sciatic nerve neuromas from rats that survived 7 and 13 d postoperatively, the interval corresponding to the peak of neuroma A-fiber hyperexcitability (Papir-Kricheli and Devor, 1988). Short segments of fixed nerve, DR, and neuroma segments were quartered longitudinally using a fresh #11 blade, and desheathed. They were then rinsed (3 × 5 min buffer, 3 × 5 min buffer with 0.1 M glycine, 4°C), transferred to blocking medium [1 × 10 min glycine/buffer containing 2% normal goat serum (Sigma), 20°C], and incubated overnight in primary antibody in blocking medium (20°C, gentle agitation).

The following day tissue was rinsed in glycine/buffer and then buffer alone (both 5 × 3 min, 20°C), incubated for 1–2 hr (20°C) in biotinylated goat anti-rabbit IgG, buffer rinsed (5 × 10 min), and reacted in ABC reagent (Elite kit, Vector Labs) followed by NiCl-intensified diaminobenzidine (DAB). Tissue was then postfixed in 3% glutaraldehyde, buffer rinsed overnight (4°C), osmicated (1% OsO_4, 4°C), dehydrated in ascending alcohols (4°C) and then propylene oxide (20°C), and embedded in LX-araldite. Longitudinal thin sections were picked up on copper grids and viewed in a JEOL 100CX. We usually avoided counterstaining and instead used a small (40 μm) aperture and low accelerating voltage (40 or 60 kV) to enhance contrast.

Antibodies. Immunolocalization was carried out using 7493, a polyclonal antibody that recognizes mammalian CNS and PNS Na^+ channels. Anti-Na^+ channel IgG was prepared by immunizing rabbits with Na^+ channel protein purified from rat brain and subsequent isolation of the IgG fraction from the serum by DEAE–Affi-Gel blue affinity chromatography as described by Elmer et al. (1990). This antibody has high affinity and selectivity for Na^+ channel protein in rat, cat, and human brain and peripheral nerve membranes. For example, in rats, it selectively recognizes the 260 kDa Na^+ channel α-peptide at dilutions up to 1:10,000 on immunoblots, 1:1000 in immunoprecipitations, and 1:200 in fluorescence immunocytochemistry (Elmer et al., 1990).

For the present experiments 7493 IgG was affinity purified by passage through a column to which purified Na^+ channel protein (specific activity > 2600 pmol ^{3}H-saxitoxin binding/mg protein) was coupled (Elmer et al., 1990). The aim was to remove from the IgG fraction any non-Na^+ channel–recognizing antibodies. Unbound IgG was removed by washing the column with Tris-buffered saline. Purified Na^+ channel–specific antibodies were then rapidly eluted with ice-cold 4 M $MgCl_2$ and diluted 100-fold with Tris-buffered saline. After dilution, the affinity-purified antibodies that emerged from the column recognized the 260 kDa Na^+ channel α-peptide at dilutions of 1:100 on immunoblots, 1:50 in immunoprecipitations, and 1:10–20 in the present electron microscopic immunocytochemical study (see Results). Thus, compensating for dilution, affinity purification somewhat improved the specific IgG titer. Biochemical characterization has confirmed that 7493 recognizes the polypeptide portion of the Na^+ channel with no reactivity toward the carbohydrate portion (K. Angelides, unpublished observations).

Tissue underwent primary incubation alternatively using 7493 IgG ("primary 7493 IgG"), or affinity-purified 7493 IgG. To monitor for nonspecific immunolabeling, control samples underwent primary incubation in the absence of any antiserum ("no primary"), by using preimmune serum from rabbit 7493 ("preimmune 7493"), or using "preabsorbed 7493 IgG" that emerged from the Na^+ channel column prior to elution of affinity purified antibodies.

Results

Overall structure of neuroma preparations

Nerve ends divided roughly into four contiguous zones (Fried et al., 1991). (1) At >3 mm proximal to the ligature, axons were largely intact, with only minor changes in diameter, and myelin and nodal structure. (2) Between 3 mm and ≈300 μm was a "zone of dysmyelination." Here, the myelin sheath of most axons was disrupted and undergoing active phagocytosis, while in others new myelin was being laid down. This zone was rich in demyelinated preterminal axon segments, swollen organelle-packed terminal "end bulbs," and at later survival times, numerous preterminal axon branches and fine unmyelinated sprouts. (3) In the 300 μm nearest the ligature was a "zone of demyelination" in which myelin was removed without renewal. Most axon end bulbs occurred within this region, which also had many demyelinated axons, and a gradually increasing population of axons sprouts. (4) Finally, under the ligature, was a "compression zone" that contained few, if any, neuronal processes. In the present study we focused on Na^+ channel immunolocalization within the zones of dys- and demyelination in the distal 3 mm of the injured nerve.

Immunolabel specificity and the heterogeneous distribution of Na^+ channel epitopes in normal axons

Specificity. Immunolabeling using 7493 IgG occurred consistently on some cell types and membrane locations, avoiding others completely (see below). There was no intracellular labeling. Primary 7493 IgG yielded the most intense immunolabeling of membranes, although with this material there was always some decoration of basal lamina (e.g., open arrow in Figs. 3*A*, 6*A*). Most of this can be attributed to antibodies present in the preimmune serum, as this labeled basal lamina with little or no binding to membranes recognized specifically by 7493 antibodies. The marking of basal lamina was essentially eliminated by affinity purification of the 7493 IgG (e.g., Fig. 3*C*).

Tissue incubated without primary antibodies, or using preimmune serum, yielded no labeling of membranes that were consistently 7493 positive, including nodes of Ranvier and sprouts (Fig. 1*E*; see Figs. 4*E*, 8*F*). In tissue exposed to preabsorbed 7493 IgG, the specific Na^+ channel signal was essentially eliminated, but the labeling of basal lamina persisted (see Figs. 3*D*, 8*D*). Typically, Na^+ channel–specific marking was discernible even in the presence of the impurity that marked basal lamina (see Figs. 3*A*, 6*A*). Nonetheless, all of the illustrations and conclusions in this article are based on the affinity purified 7493 IgG, except in the few instances specifically noted.

Nodes of Ranvier. To gain confidence in our immunolabeling regimen, we began by examining nodes of Ranvier. Nodal axolemma is known from electrophysiological, biochemical, and structural (affinity and immunoprobe) studies to be rich in Na^+ channels (Waxman and Ritchie, 1985). Within the zone of antibody penetration the nodal membrane of *all* nodes showed heavy immunolabeling using primary or affinity-purified 7493 IgG (Fig. 1*B–D*; see Fig. 8*E*). Moving from nodal to paranodal membrane, there was a sharp boundary, marked by the last adaxonal paranodal Schwann cell loop, beyond which there was no detectable labeling whatsoever. Similarly, internodal axolemma was never marked (e.g., Figs. 1*C,D*; 4*C*; 8). We did not recognize any obvious differences between 7493 labeling of nodes in intact axons versus those proximal to neuromas, or between nerve and DR preparations.

Schwann and other non-neural cells. The limiting membrane of Schwann cells was consistently 7493 positive, albeit much less intensely so than nodal axolemma. Labeling was roughly homogeneous (not patchy), and it was of similar intensity on Schwann cell membrane external to myelin, at paranodal loops, and on the mesaxonal sheaths surrounding bundles of unmyelinated axons (e.g., Fig. 1*C*, small arrow; see Fig. 4). Compact myelin itself, including the innermost layer adjacent to inter-

nodal axolemma, was not labeled. Adjacent to nodes and at Schmitt-Lantermann incisures, at least, lanthanum has access to these targets (Mackenzie et al., 1984). Since this tracer is thought to move in the form of colloidal $La(OH)_2$ with dimensions similar to those of IgG molecules (Revel and Karnovsky, 1967), antibody access is not unlikely. These membranes also failed to label in experiments in which they were fully exposed and access was unequivocal (see below, Fig. 8).

In some axons, paranodal Schwann cell "brush border" villi occupy the nodal gap (Berthold and Rydmark, 1983). Interestingly, the distal ends of these villi, adjacent to the axolemma, appeared to label heavily (Fig. 1*A,B*). Macrophages (Fig. 2) and vascular endothelial cells were consistently immunonegative.

Na^+ channel accumulation, and axolemmal remodeling in neuromas

Axonal branch points. Within the zone of dysmyelination we occasionally encountered axon bifurcations. Most were Y-shaped, where the stem branch was the larger in diameter and had the more mature-looking myelin, as might be expected of the parent axon (p in Fig. 9*A*). The two daughter branches were of smaller diameter, and one or both were either unmyelinated, or had thin myelin suggestive of recent (re)myelination (d_1, d_2 in Fig. 9*A*). The Y-shaped nodal axolemma was heavily labeled with 7493 IgG up to the beginning of the myelin sheath. On daughter branches that were not myelinated, axolemmal labeling continued, if at substantially reduced intensity, under the enveloping layer of Schwann cell cytoplasm. Labeling along these branches was much like that associated with demyelinated preterminal axon branches.

Demyelinated preterminal axon branches. We frequently encountered relatively large-diameter (>1 μm) axons, stripped of myelin, on which active macrophages still adhered (Fig. 2). Loops of basal lamina left over from the original myelinating Schwann cell were usually visible externally (e.g., inset in Fig. 2*A*). On the basis of the stage of myelin debris breakdown in digestion vacuoles in the cytoplasm of these macrophages (dv in Fig. 2*A,B*) one could roughly gauge how recently demyelination had taken place (Beuche and Friede, 1986; Fried et al., 1991).

In early demyelination, when myelin lamellae could still be recognized in the intravacuolar debris, axolemma under the macrophage soma was usually 7493 negative. Moving out from under the macrophage toward regions ensheathed by Schwann processes, however, the axonal membrane was labeled. There was no indication of a diffusion (access) barrier where label began, suggesting that this gradient of 7493 labeling reflected a true gradient in the density of Na^+ channels (Fig. 2*A*). In axons where myelin digestion was more advanced, presumably indicating the passage of more time since myelin removal, axolemmal labeling was seen also under the macrophage (Fig. 2*B*).

Large-diameter axons (>1 μm) that had lost their myelin also occurred without an adherent macrophage, especially in the zone of demyelination ≤300 μm from the nerve end. These were always ensheathed by Schwann cell processes with loose loops of residual basal lamina externally (arrow in Fig. 3*C,D*). The axolemma of many of these axons labeled evenly or patchily with 7493 (Fig. 3). Although less dense than at nodes, the labeling was distinct; clearly different from the lack of axolemmal labeling underneath compact myelin. Some demyelinated axons appeared not to be labeled even though nearby ones clearly were (Fig. 3*F*, a_1 vs a_2).

Fine unmyelinated axons and axon sprouts. In intact nerve regions unmyelinated axons (<1 μm diameter) ran in parallel "Remak" bundles, with individual axons separated by a mesaxonal sheath (a lamella of Schwann cell cytoplasm). The entire bundle, which typically contained 5–20 axons, was wrapped externally by a Schwann cell (Berthold, 1978). Within neuromas, some of the axons in such bundles were closely apposed (separated by an ≈130 Å cleft without an intervening glial process), and they often appeared to be intertwined rather than parallel (Fig. 4*A,D*). Many such profiles were probably outgrowing sprouts.

The axolemma of fine neuroma fibers was almost always 7493 positive, usually in a continuous manner, but sometimes in patches. This was so whether or not mesaxonal wrapping was present (Fig. 4). Labeling intensity was usually greater than that of nearby large-diameter demyelinated axons, but it was clearly less than nodal axolemma. As with demyelinated axons, there was individual variability in labeling intensity, even among neighboring fibers in a bundle (e.g., Fig. 4*A,B*).

The membrane of unmyelinated axons within apparently normal Remak bundles was also immunopositive. Our impression was that these fibers tended to be less intensely labeled than neuroma sprouts (compare Fig. 4*A,D* with 4*B,C*). However, due to variability in the tissue samples, and the generally nonquantitative nature of DAB-based immunohistochemistry, we hesitate to draw a firm conclusion.

Neuroma end bulbs. End bulbs were instantly distinguishable from preterminal axon segments due to the composition of their cytoplasm (Figs. 3*A*, eb; 5–7), densely packed with membrane-

→

Figure 1. Na^+ channel immunolabeling with antibody 7493 at normal nodes of Ranvier from rat DR L4,5 axons. *A*, Tangential section through "brush border" villi near the nodal axolemma. *Arrows* indicate immunolabeling on villi and paranodal Schwann cell membrane. *B*, Longitudinal section through a node (same axon as in *C*) showing detail of labeled "brush border" villi and axolemma. *C*, Longitudinal section through a node. Labeled nodal axolemma and Schwann cell membrane are indicated by *large* and *small arrows*. *D*, 7493 immunolabeling of a node without "brush border" villi. *E*, Control tissue showing absence of nodal staining using preimmune 7493 IgG (*arrows*). Tissue in all of the figures was processed with affinity-purified 7493 antibody diluted 1:10 or 1:20 except where noted otherwise. Scale bars, 1 μm.

Figure 2. *A*, A macrophage (*m*), filled with fresh myelin-filled digestion vacuoles (*dv*), has recently demyelinated this axon (*a*). The *inset* highlights the area of transition from 7493-immunonegative to immunopositive (*solid arrow*) axolemma. Labeling follows the axolemma, not the macrophage (*open arrows*). *B*, Like *A* but myelin breakdown within digestion vacuoles (*dv*) is more advanced. There is now 7493 immunolabeling on the axolemma under the adjacent macrophage soma (*arrows*). The membrane of the macrophage itself is immunonegative. 7 d DR neuroma. Scale bars, 1 μm.

Figure 3. 7493 immunolabeling of demyelinated preterminal axons (diameter > 1 μm). *A* shows several immunopositive axons, one ending in a neuroma end bulb (*eb*). For this image, primary 7493 IgG was used, accounting for the weak labeling of the basal lamina (*open arrow*). *B* and *C*, Patchy labeling of axolemma (*small arrows*). Affinity-purified 7493 was used, and loose residual basal lamina loops (*open arrow*) are immunonegative. *D*, Using preabsorbed 7493, basal lamina was labeled (*open arrow*), but not axolemma (Fig. 8*D*). *E*, Transverse section showing three labeled axons that are closely apposed (a_1, a_2, a_3). The numerous mitochondria in a_2 suggest proximity to the axon's end bulb. *F*, Longitudinal section through two closely apposed axons. Only one of the two (a_2) is immunopositive (*arrows*). *A–D* and *F*, 7 d DR neuromas; *E*, 13 d DR neuroma. Scale bars, 1 μm.

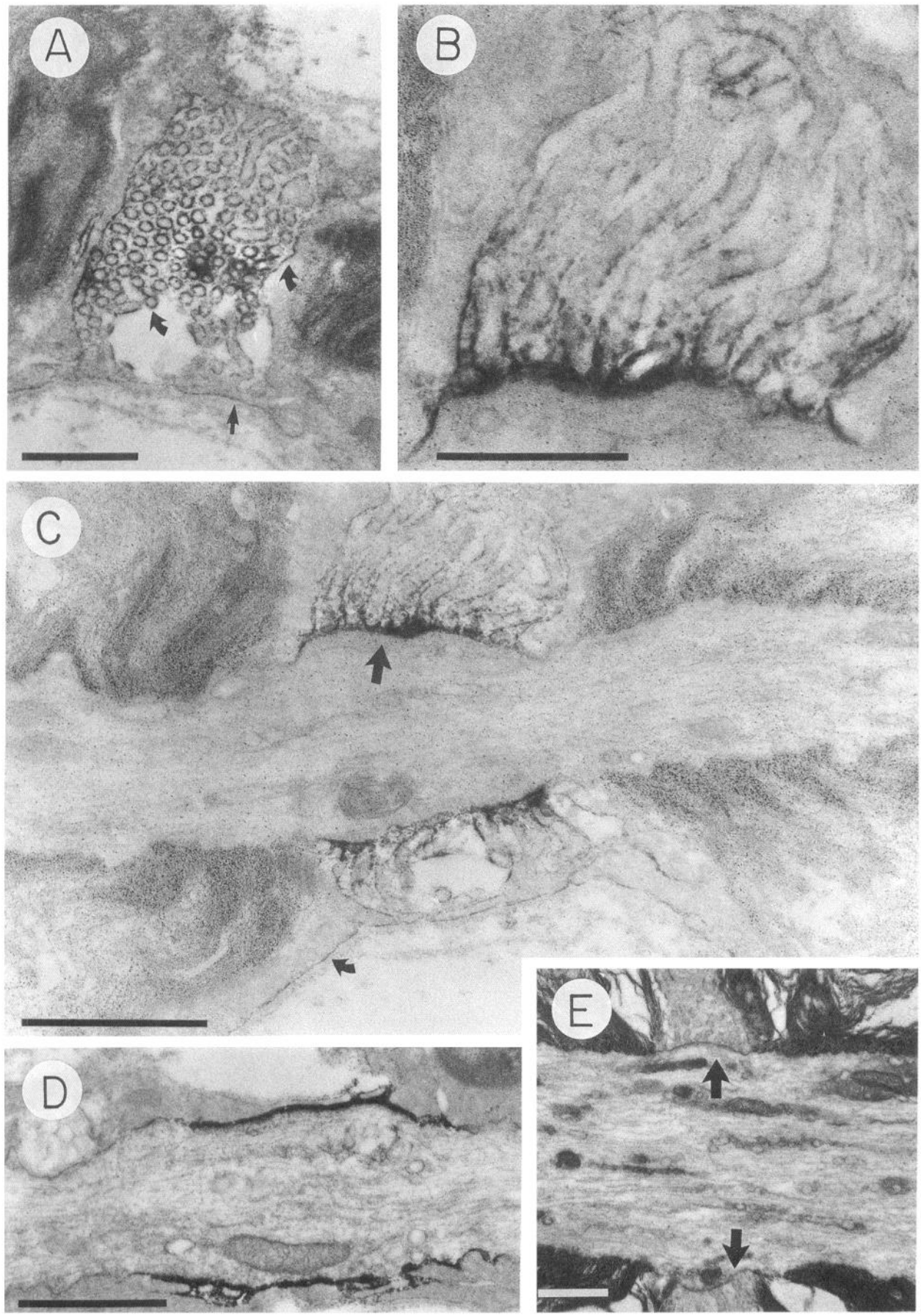
A
B
C
D
E

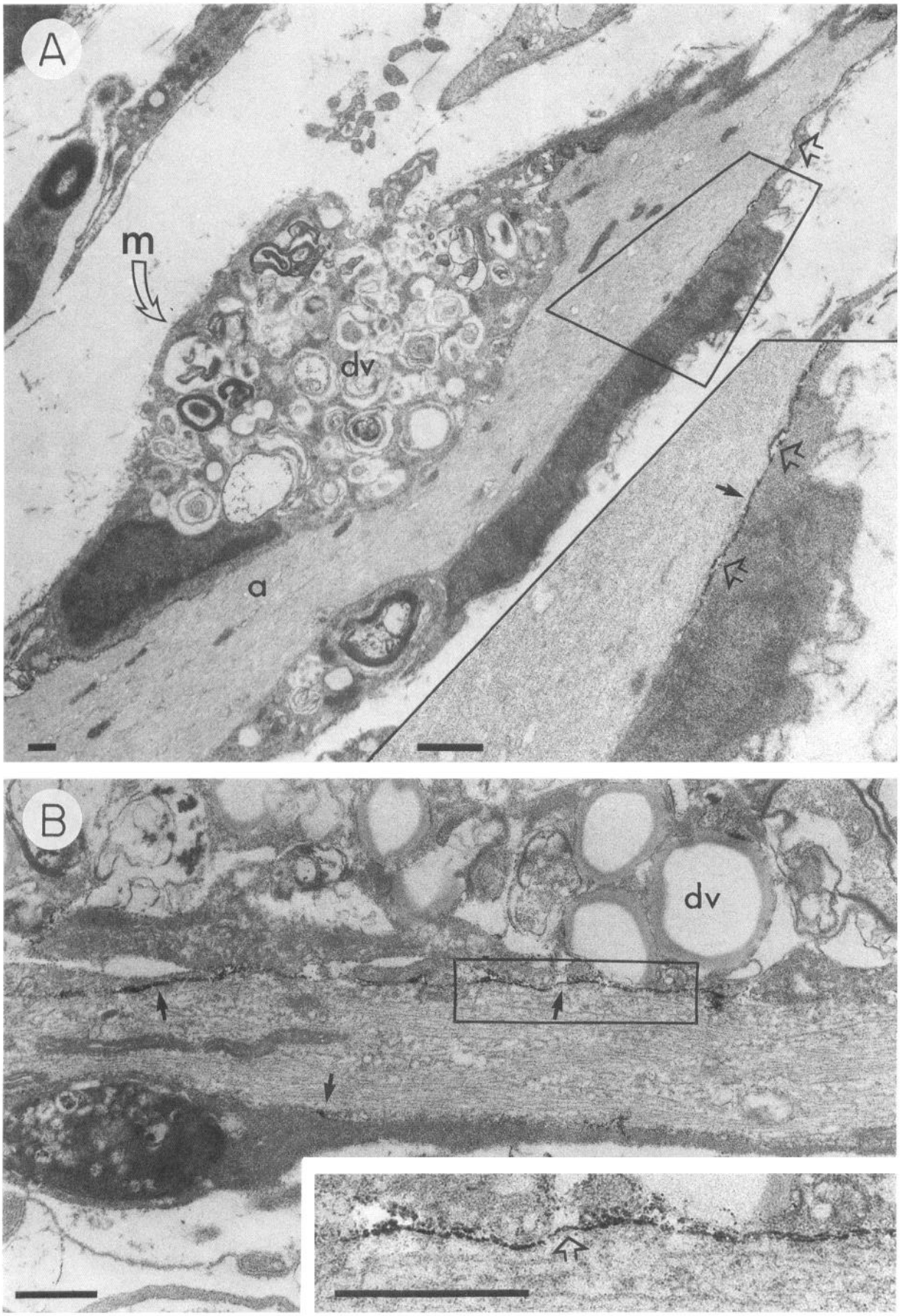
A
m
dv
a
B
dv

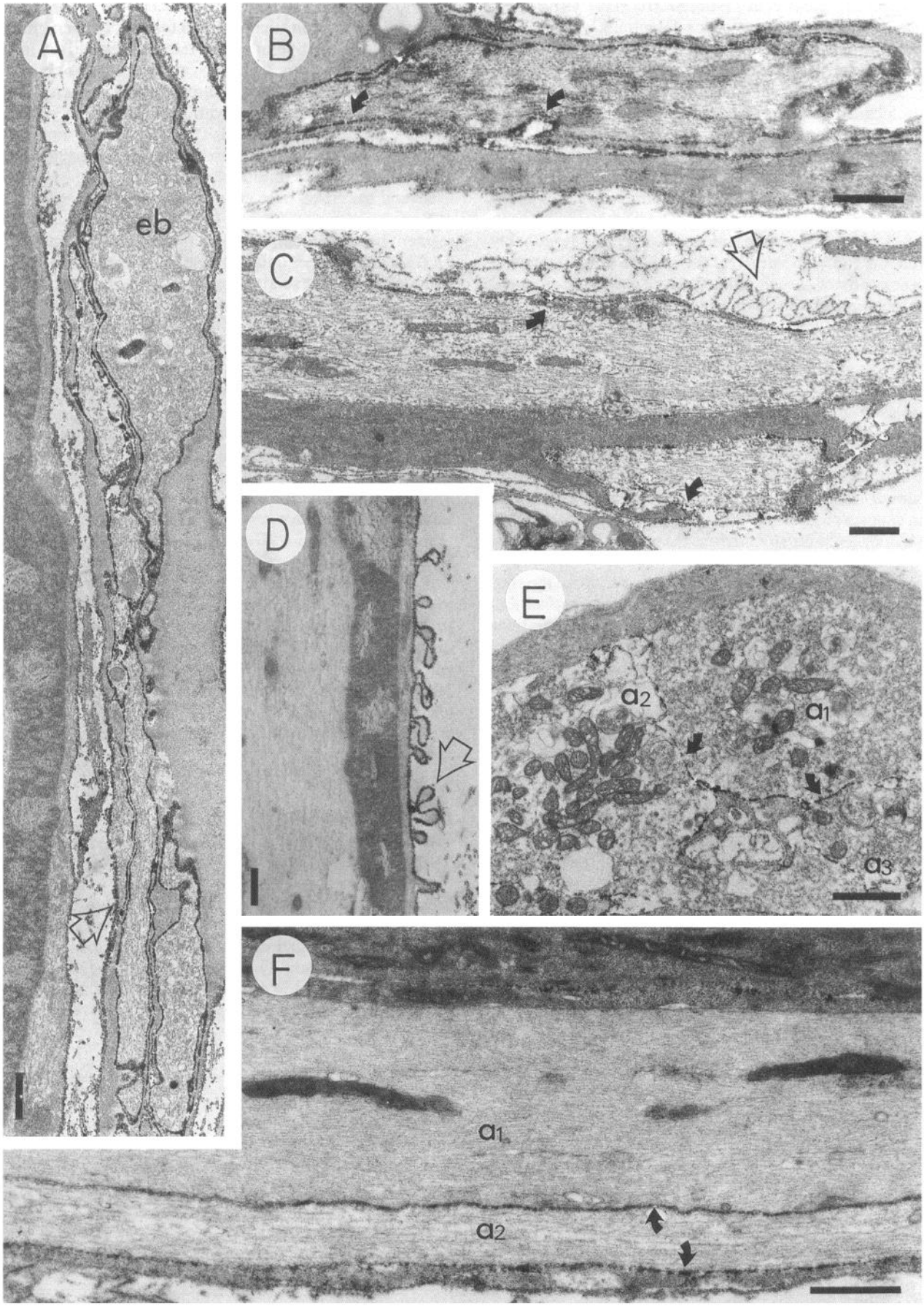
A
eb
B
C
D
E
a2
a1
a3
F
a1
a2

bound organelles (Zelena et al., 1968; Morris et al., 1972; Fried et al., 1991). Virtually all were circumferentially wrapped in a thin sheath formed of one, or sometimes a few lamellae of Schwann cell cytoplasm, covered externally by basal lamina.

The axolemma of most end bulbs was labeled with 7493 IgG, usually in localized patches (Figs. 5–7). Labeling intensity was similar to that associated with demyelinated preterminal axon branches, although individual patches sometimes labeled quite heavily. In favorably oriented end bulbs the stem axon was visible. Usually this had the labeling characteristics of a demyelinated (> 1 μm) or unmyelinated (< 1 μm) preterminal axon (e.g., Figs. 3*A*, 5*A*, 6*D*). A fine stem axon (e.g., Fig. 5) probably means that the end bulb formed at the end of a fine parent axon (e.g., a nociceptive C-fiber), although such a stem axon could also be a preterminal sprout of a myelinated parent axon. Occasionally, compact myelin and a 7493-labeled heminode identified the end bulb unequivocally as belonging to an A-fiber (Fig. 7). Moving from the heminode in the direction of the end bulb, the intensity of 7493 labeling always fell off, but in most cases label persisted onto the axolemma of the short demyelinated stem axon and the end bulb itself.

In a significant minority of end bulbs (≥30%) the axolemma was not recognizably labeled, even though adjacent 7493-positive nodes of Ranvier and Schwann cells confirmed that there had been exposure to the 7493 antibody (Fig. 7). Failure to label was not associated with any obvious peculiarity of the axon or its glia.

Acutely cut axon ends. For comparison, we examined the ends of some normal axons that had been cut acutely (after fixation) and then incubated in primary 7493 IgG. In these preparations the axon membrane was breached, and the cytoplasm and axolemma were freely accessible to the incubation medium. Myelin at the cut end was sometimes torn from the axon, and usually it was macerated (Fig. 8*A–C*). Its presence, however, was sufficient to identify the transection site as internodal.

The cytoplasm was diffusely labeled for about 10 μm from the cut end (Fig. 8*A,B*). However, we hesitate to ascribe this to intracytoplasmic Na^+ channels, as similar, but weaker, labeling also appeared in tissue incubated with preimmune antiserum (Fig. 8*C*). There was a hint of preferential marking of neurofilaments and neurotubules, the subaxolemmal filamentous matrix, and small lucent vesicles (Fig. 8*A,B*). More salient to the present topic was the observation that neither the external face of the (internodal) axolemma, the adjacent face of Schwann cell membrane, nor exposed leaves of compact myelin labeled (Fig. 8*A,B*). Acute transection clearly provided the antibodies with access to these membrane surfaces. Positive labeling of nearby nodal axolemma (Fig. 8*E*) confirmed adequate tissue processing.

Remyelination. As noted above, there were axons in chronic neuroma preparations that had well formed, but very thin compact myelin suggestive of recent remyelination. This interpretation is supported by the observation of similar thin myelin on the daughter branches of bifurcating neuroma axons (d_1 and d_2 in Fig. 9*A*), and on axons with very closely spaced nodes of Ranvier (Fig. 9*C*; Hildebrand, 1989). Whenever compact myelin was present, including these axons, the underlying axolemma was free of 7493 immunolabeling.

Several examples were encountered of closely spaced nodes of Ranvier with a very short (tens of micrometers) internodal segment between them, occupied by a single Schwann cell (Fig. 9*B,C*). This configuration is typical of the early stages of myelin remodeling in regenerating and remyelinating axons (Hildebrand et al., 1986; Hildebrand, 1989). As remyelination proceeds, the Schwann cells on the short internodes are excluded, and the two adjacent internodes expand until they meet at a new shared node of Ranvier. This implies the dynamic remodeling of axolemmal channel content, a process we believe we have captured in Figure 9, *B* and *C*.

Figure 9*C* shows two well-formed nodes of Ranvier (arrows) with a short (10 μm) intercalated Schwann cell that has formed about five lamellae of adaxonal myelin (arrow m). Na^+ channel immunolabeling is restricted to the nodes and does not extend under any of the three segments of para/internodal axolemma that are visible. Figure 9*B* is similar, except that the intercalated Schwann cell appears to be withdrawing. No myelin is present, and patches of axolemma have been abandoned and exposed to the extracellular medium. Significantly, both the exposed patches of (formerly internodal) axolemma, as well as axolemma under the remnants of the Schwann cell, are 7493 positive (straight arrows, Fig. 9*B*). This labeled membrane forms a bridge 10 μm in length between the two labeled nodes of Ranvier (curved arrows). If the process were to proceed to completion (unlikely in a neuroma), a single mature node might eventually form at this location.

Discussion

Immunolocalization

We have used a newly developed polyclonal anti-Na^+ channel antibody, 7493, to immunolocalize Na^+ channels in membranes of normal peripheral nerve axons, and to assess remodeling following nerve section and neuroma formation. Our main aim was to determine whether nerve injury triggers changes in axolemmal Na^+ channel distribution that could account for the ectopic hyperexcitability of afferent axon endings trapped in neuromas. With this in mind, nerve/DR samples were taken at the time of peak neuroma hyperexcitability (Devor, 1993). We

→

Figure 4. Small-diameter unmyelinated axons and sprouts. *A*, A rope of fine immunopositive axons, probably neuroma sprouts. *B*, Transverse section through a bundle of unmyelinated axons within a mesaxonal sheath. Some are (weakly) 7493 positive (e.g., *arrows*) and some are not. *C*, An unlabeled myelinated axon (a_1, *open arrow*) beside two labeled nonmyelinated axons (a_2, a_3, *solid arrows*). In both cases the ensheathing Schwann cell membrane is weakly labeled. *D*, A bundle of fine immunopositive axons, many of which are in intimate contact. *E*, Membrane labeling is absent in this bundle of sprouts (like *D*) from a control neuroma sample incubated in preimmune 7493 serum. *A*, *C*, and *D*, 13 d DR neuroma; *B* and *E*, 13 d sciatic nerve neuroma. Scale bars: *A–C* and *E*, 1 μm; *D*, 0.5 μm.

Figure 5. Neuroma end bulb with patchy 7493 immunolabeling (*arrows*). A segment of the preterminal axon (*inset in A*) and the end bulb itself (*B*) are shown at higher magnification. 7 d DR neuroma. Scale bars, 1 μm.

Figure 6. Neuroma end bulbs. Sample areas of 7493 membrane immunolabeling are indicated by *arrows*. *A*, A large end bulb. In this panel (only) primary 7493 IgG was used. Note marking of loose basal lamina remnants (*open arrow*). *B* and *C*, In some places the Schwann cell sheath has separated from the end bulb membrane (*some arrows, asterisk,*) confirming independent labeling of the axolemma. *D*, Long, spindle-shaped end bulb with demyelinated stem axon. The framed part of the end bulb is enlarged in *E*. *A*, *D*, and *E*, 7 d DR neuroma; *B*, 13 d sciatic nerve neuroma; *C*, 13 d DR neuroma. Scale bars, 1 μm.

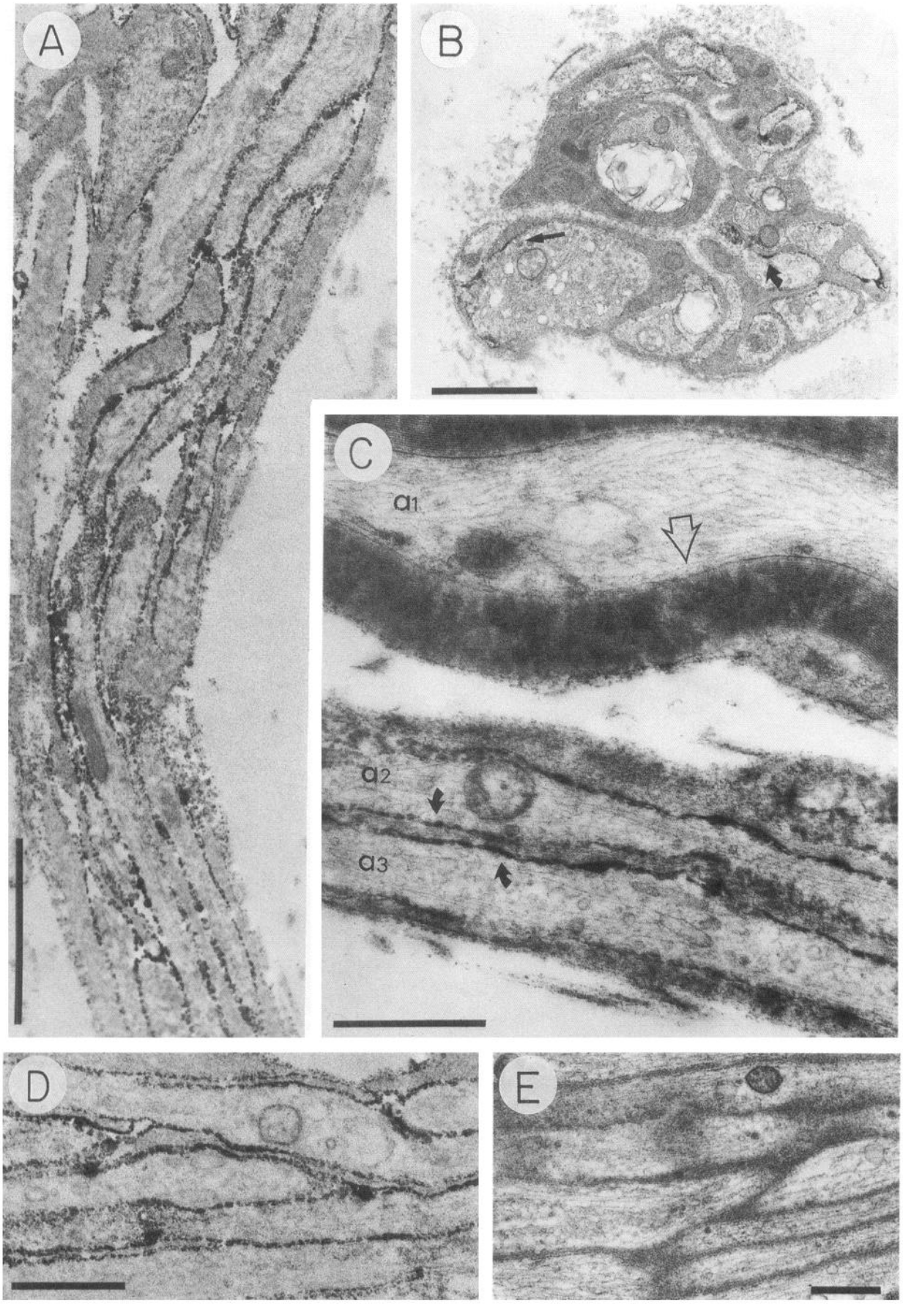
A
B
C
a1
a2
a3
D
E

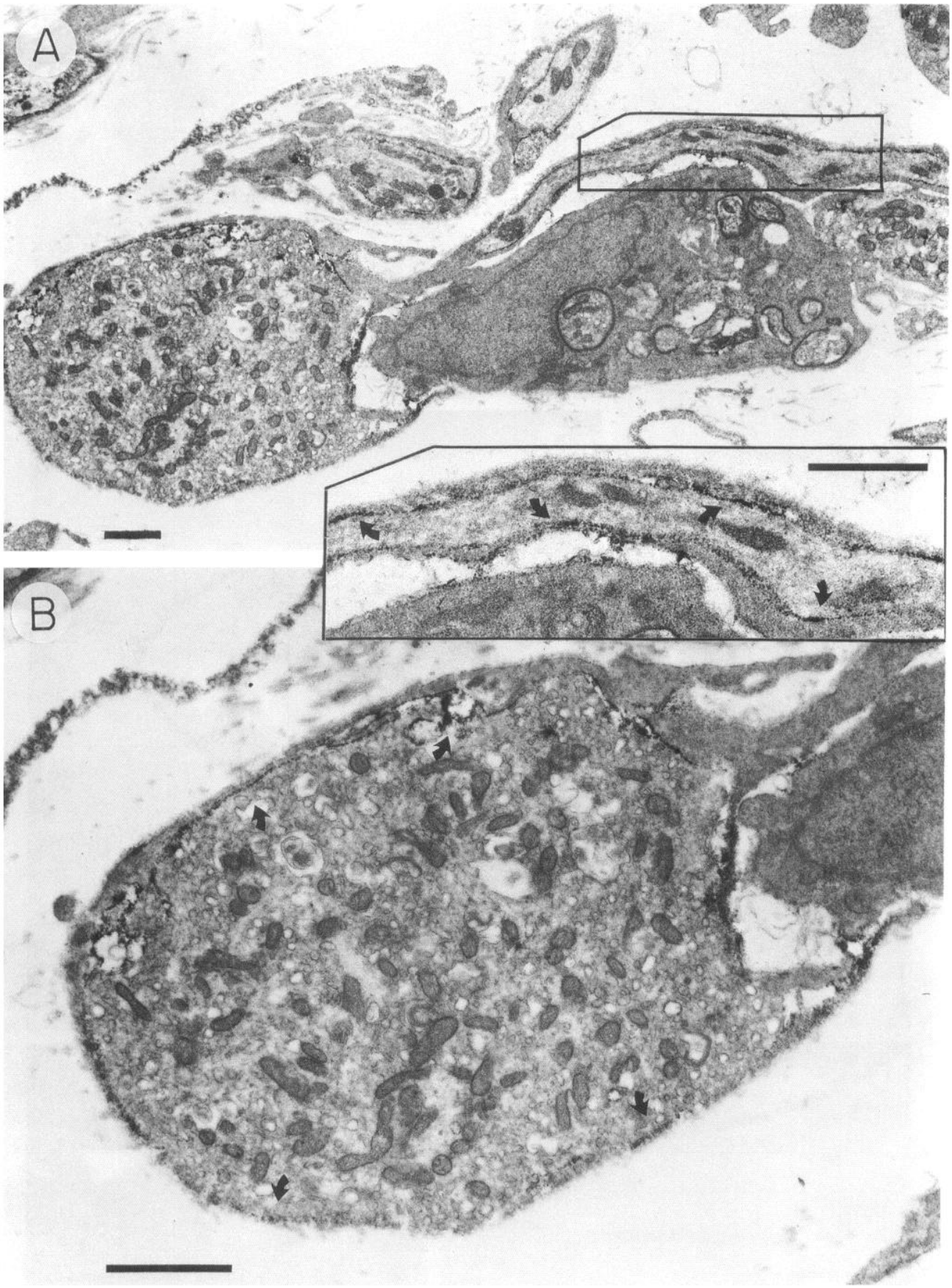
A
B

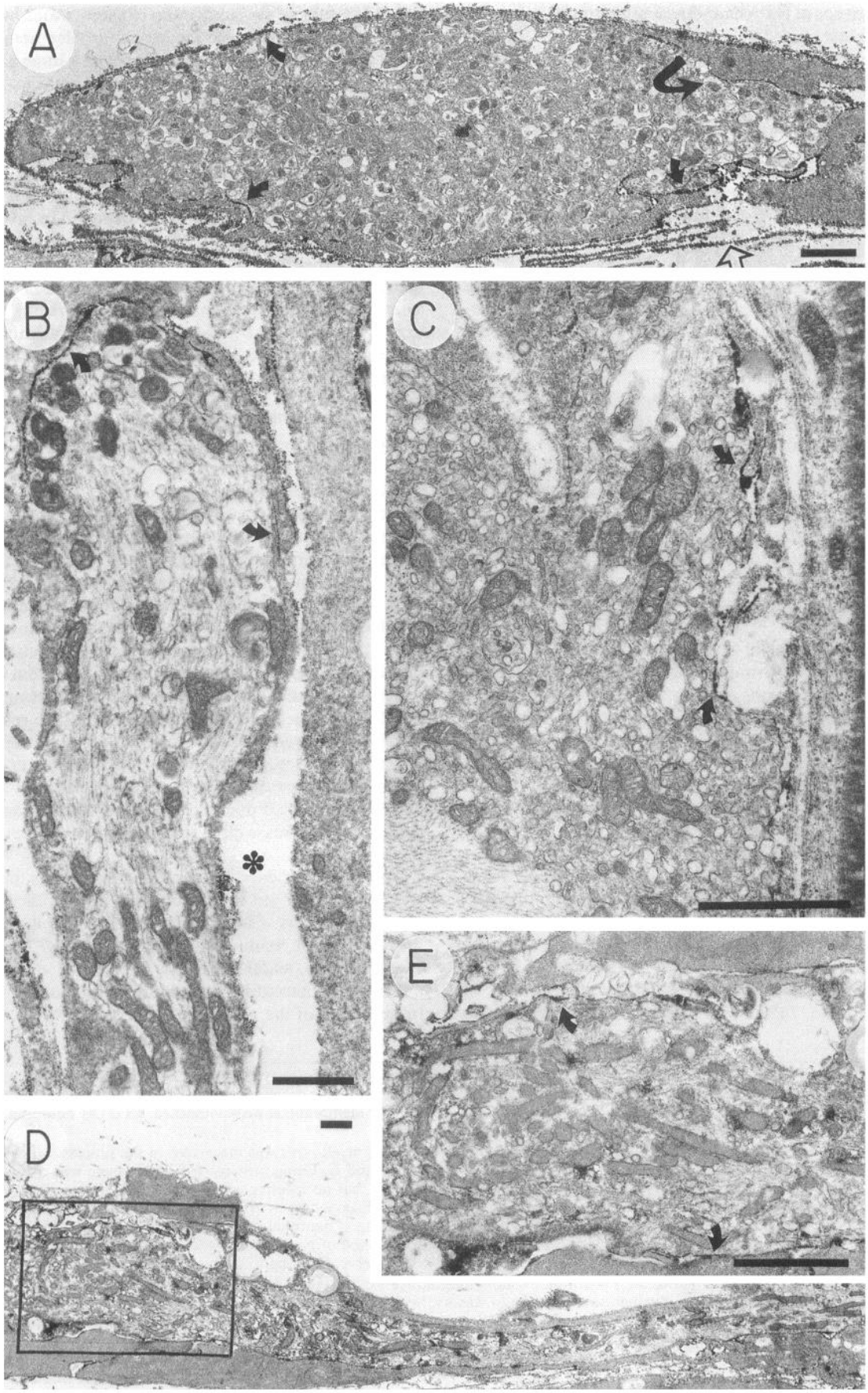
A
B
C
D
E

found clear evidence of Na^+ channel accumulation in neuromas, especially in demyelinated axons and end bulbs.

The specificity of 7493 for marking Na^+ channels in mammalian peripheral nerve has been demonstrated previously on the basis of immunoblotting, immunoprecipitation, and immunolabeling experiments (Elmer et al., 1990). The present study extends these data by showing that (1) affinity-purified 7493 selectively marks membranes known to contain Na^+ channels at significant densities, and (2) it fails to mark membranes that do not. Consistent with earlier observations using 7493 and other Na^+ channel markers (Ellisman and Levinson, 1982; Haimovich et al., 1984; Waxman and Ritchie, 1985; Black et al., 1990; England et al., 1990; Ritchie et al., 1990), as well as ample electrophysiological and biochemical data (reviewed by Waxman and Ritchie, 1985), we found that the axolemma at nodes of Ranvier is heavily labeled. On the other hand, macrophage and endothelial cell membranes were 7493 negative, as was para- and internodal axolemma even though a low density of Na^+ channels (<4% of nodal density) appears nonetheless to be present in the latter two (Grissmer, 1986; Chiu and Schwartz, 1987). It could be argued that the failure to label internodal membrane resulted from inability of the antibodies to gain access to the space between compact myelin and the axolemma. However, even when this space was opened and access assured (early stages of demyelination and acute nerve cut), the axolemma remained immunonegative (Figs. 2*A*, inset; 8*A,B*).

Also consistent with extensive prior evidence (Gray and Ritchie, 1985; Barres et al., 1990; Black et al., 1990; Ritchie et al., 1990) was our observation of weak 7493 immunolabeling of the limiting membrane of Schwann cells. The apparently intense labeling of the adaxonal ends of paranodal "brush border" villi (Fig. 1*A,B*) suggests a special role for this complex in the regulation of the local ionic milieu (Berthold and Rydmark, 1983; Gray and Ritchie, 1985). However, although we believe this indicates a high density of Na^+ channels, we cannot rigorously exclude the possibility of artifactual diffusion of DAB reaction product from the nearby nodal membrane.

Tissue samples were incubated in 7493 antibody after aldehyde fixation, but without membrane permeabilization. These conditions are expected to exclude active (endocytotic) and passive (leak) entry of antibody into the cytoplasm. Indeed, except in preparations in which we imaged axon ends cut acutely after fixation, we did not see intracytoplasmic immunolabeling with 7493 in any cell type (Ritchie et al., 1990).

On the other hand, 7493 labeling was consistently present on the axolemma of de- and unmyelinated axons, sprouts, and neuroma end bulbs. Since the axonal profiles were usually adjacent to Schwann cells or macrophages, it is important to assure that the labeling was indeed associated with the axolemma. We can be certain of this for two reasons. First, adjacent membranes occasionally separated for short distances. When such gaps occurred between a neuron and a Schwann cell, it was clear that both membranes were labeled (e.g., arrows in Figs. 3*B,C*; 4). At gaps between neurons and macrophages, labeling clearly followed the neuron (Fig. 2*A,B*, open arrows in insets). Second, as has been noted previously (Bernstein and Pagnanelli, 1982; Devor and Bernstein, 1982; Vahle-Hinz et al., 1987), there were many instances in which a Schwann cell ensheathed two or more axons or end bulbs as a unit, with no intervening glial process (e.g., Figs. 3*E,F*; 4*A,D*). Labeling where the membrane of such adjacent axons touched guarantees that at least one was immunopositive.

Demyelination and remyelination

Many large-caliber axons were stripped of myelin by activated macrophages. The exposed axolemma was unlabeled in cases where the state of intravacuolar digestion of myelin debris in the macrophage indicated that myelin removal had occurred recently. Where more time had elapsed and vacuolar digestion was more advanced, the axolemma was 7493 positive. Likewise, only a short distance away from the macrophage, where the axon had presumably been denuded of myelin some time earlier, the axolemma had already acquired 7493 immunoreactivity (Fig. 2). These observations indicate that Na^+ channel density increases in a spatial (and temporal) gradient from less to more recently demyelinated regions. Similar remodeling of axolemmal Na^+ channel content was evidenced in the removal of intercalated Schwann cells during the process of remyelination, and at bifurcation points in branched neuroma axons (Fig. 9). We interpret these observations to mean that local Na^+ channel density is regulated dynamically; in para- and internodal axolemma it can increase quite rapidly (days or perhaps hours) after myelin removal.

Even in the absence of attached macrophages, unmyelinated axon profiles >1 μm in diameter can be identified as formerly myelinated fibers. Could the observed 7493 labeling in such fibers represent residual nodal Na^+ channels? In normal myelinated axons, nodal axolemma is only 1–2 μm in length, has a distinct undercoating, and occupies only about 0.1% of the linear extent of the axon (Fig. 1; Berthold, 1978). Since much

→

Figure 7. *A*, Large neuroma end bulb that has formed adjacent to a labeled heminode. Note myelin (*m*) of the first internode to the *left*, and the soma of the ensheathing Schwann cell (*far right*). *B*, Higher magnification of the end bulb showing heavy labeling of axolemma at the heminode (*arrows*), but virtually none of the adjacent end bulb axolemma. The Schwann cell membrane is weakly marked. 13 d DR neuroma. Scale bars, 1 μm.

Figure 8. Ends of axons that were cut acutely prior to immunostaining. Note that myelin (*m*) was macerated in the process, exposing internodal axolemma, internal myelin leaflets, and the inner Schwann cell membrane. *A, B,* and *E*, Using primary 7493 IgG, there was diffuse cytoplasmic labeling, with a hint of labeling of (some) cytoplasmic vesicles (*open arrow in B*), but no labeling of axolemma (*solid arrows*), myelin, or inner Schwann cell membranes. The immunopositivity of axolemma at nearby nodes of Ranvier (*open arrow in E*) confirms adequate processing. *C* and *F*, Preimmune 7493 IgG yielded weak diffuse cytoplasmic labeling, and no labeling of neuronal or Schwann cell membranes, including at nodes of Ranvier. *D*, Nodal axolemma failed to label using preabsorbed antiserum, depleted of Na^+ channel–recognizing antibodies. *Arrowheads* in *D–F* indicate the limits of nodal axolemma. *A, B,* and *E*, DRs; *C, D,* and *F*, sciatic nerve. Scale bars, 1 μm.

Figure 9. Branch points and remyelination in a neuroma. *A*, Longitudinal section through a bifurcation in which a myelinated parent axon (*p*) yields two newly (thinly) myelinated (*m*) daughter branches (d_1, d_2). Heavy 7493 immunolabeling of the axolemma at the complex node of Ranvier (*arrows*) falls off sharply at the perinodes. *B*, Two closely spaced immunopositive nodes (*curved arrows*). The intervening axolemma, which is associated with an apparently withdrawing Schwann cell and no myelin, is weakly labeled (*straight arrows*). As often occurs at such sites (Morris et al., 1972; Hildebrand et al., 1986; Chan et al., 1989; Hildebrand, 1989), part of the axon in this area is swollen and vacuolated (*asterisk*). *C*, The Schwann cell between this pair of closely spaced nodes of Ranvier (*curved arrows*) has formed a thin layer of myelin (*m*), and the subjacent axolemma is 7493 negative. *A* and *C*, 13 d DR neuroma; *B*, 7 d DR neuroma. Scale bars, 1 μm.

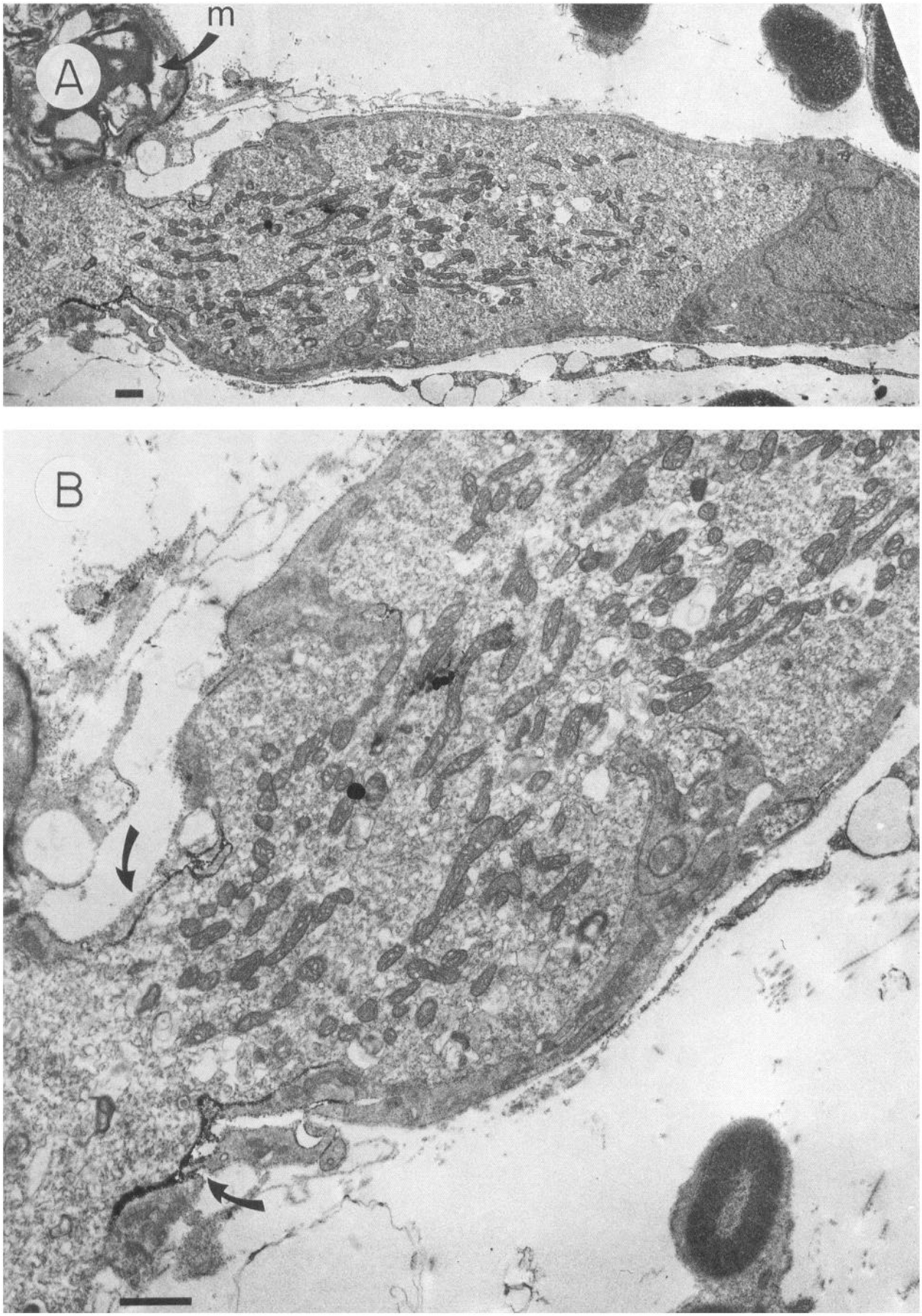
m
A
B

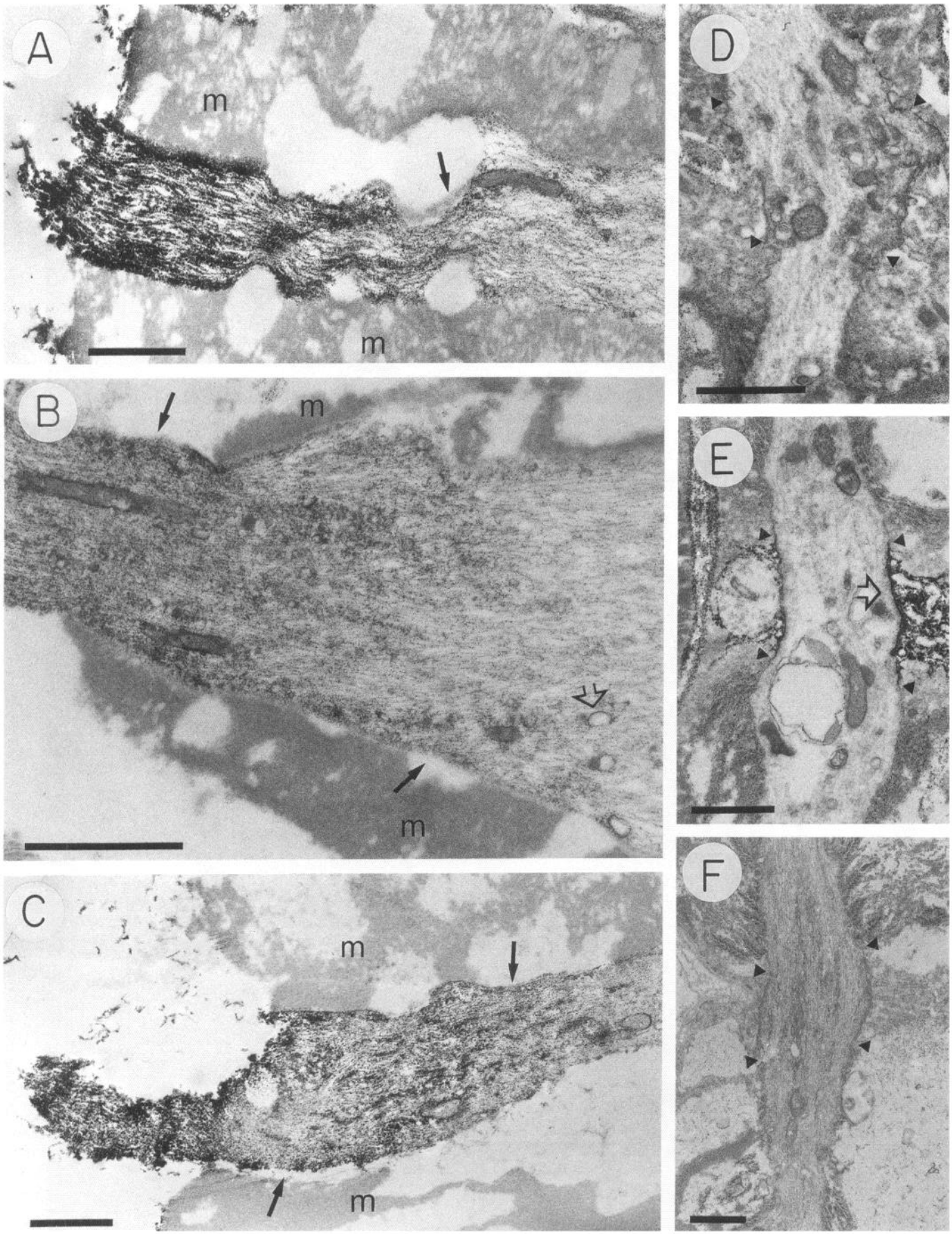
A
m
m
B
m
m
C
m
m
D
E
F

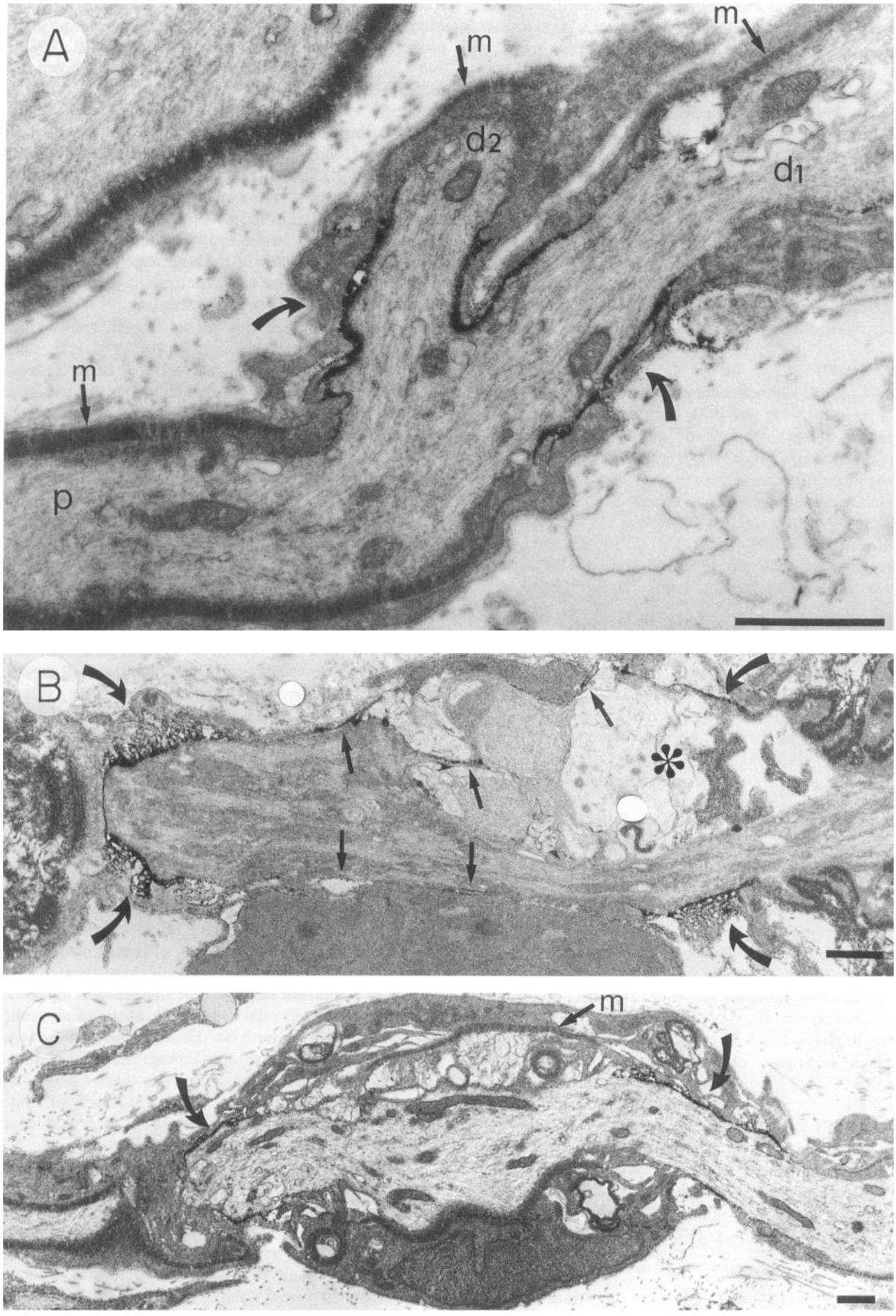
A
m
m
m
d2
d1
p
B
*
C
m

longer stretches of labeled axolemma were often seen, and they did not have an undercoat, they could not all have been former nodal axolemma. We conclude that myelin stripping triggers/permits the insertion (accumulation) of Na^+ channel proteins that were not there previously, resulting in a net increase in Na^+ channel density. The identical argument also holds for end bulbs.

Axon sprouts

Unmyelinated neuroma profiles <1 μm in diameter, which include mature unmyelinated axons, sprouts, and perhaps shrunken demyelinated axons (Aitken and Thomas, 1962), were usually 7493 positive. Indeed, their immunolabeling tended to be more intense than that of large-diameter profiles. Unfortunately, the methods used did not permit us to establish whether the Na^+ channel density of neuroma sprouts was significantly increased from that of unmyelinated axons in normal nerve.

Neuroma end bulbs

The evidence of Na^+ channel accumulation on end bulb axolemma is consistent with our prior light and electron microscopic evidence of Na^+ channel immunolocalization in neuromas in the lateral line nerve of *Apteronotus* using fish-specific anti-Na^+ channel antibodies (Devor et al., 1989). Likewise, since Na^+ channels yield large-diameter intramembranous particles (IMPs) in freeze-fracture replicas (Ellisman, 1979; Ellisman et al., 1983; Rosenbluth, 1983; Small et al., 1984; Stricharz et al., 1984), it is consistent with the observed shift of IMP sizes in rat neuroma end bulb axolemma to larger values (Fried et al, 1991).

Unlike neuroma sprouts and Schwann cells, large-caliber demyelinated axons and neuroma end bulbs often showed patchy 7493 labeling. Axolemma at the edges of immunopositive patches appeared the same as contiguous unlabeled axolemma, and glial ensheathment at these borders was unremarkable. We therefore presume that the patchy immunolabeling indicates true patchy distribution of Na^+ channels. This may reflect regional channel insertion (see below) with limited mobility in the membrane plane (Angelides et al., 1988; Joe and Angelides, 1992, in press). Alternatively, mobile channels may have been trapped by subaxolemmal anchoring molecules not resolved in our material (Pappone and Cahalan, 1985; Srinivasan et al., 1988; Kordel et al., 1990).

Even in tissue areas where the adequacy of antibody access and immunocytochemical processing were unequivocal, at least 30% of demyelinated preterminal axons and neuroma end bulbs were not immunolabeled with 7493 IgG (e.g., Figs. 3*E,F*; 7). We propose that this indicates intrinsic variability among different functional classes of axons. For example, among injured afferents the likelihood and frequency of spontaneous ectopic firing is related to sensory receptor type (Devor et al., 1990; Johnson and Munson, 1991; Koschorke et al., 1991). Likewise, injured somatic and presumably postganglionic sympathetic *motor* axons rarely generate ectopic discharge (Devor, 1993). On the grounds that ectopic electrogenesis appears to be a direct consequence of axolemmal Na^+ channel accumulation (see below), the 7493-negative profiles may simply represent neurites of motor neurons (sciatic neuromas), and/or afferent types that do not develop hyperexcitability (sciatic or DR neuromas).

The process of Na^+ channel incorporation in neuromas

Na^+ channel protein is synthesized in the cell soma (Schmidt and Catterall, 1986; Brismar and Gilly, 1987) and conveyed from there to the axon end. Over short distances Na^+ channels might migrate by lateral diffusion in the membrane plane (Pfenninger, 1982; Small et al., 1984; Strichartz et al., 1984; but see Joe and Angelides, 1992, in press). However, given their brief half-life (probably 1–3 d; Schmidt and Catterall, 1986; Brismar and Gilly, 1987), and their heterogeneous, rather than gradient-like, distribution along (myelinated) fibers many centimeters in length (Waxman and Ritchie, 1985), this transport mechanism is precluded. Rather, like most membrane-bound proteins, Na^+ channels are presumably conveyed by rapid axoplasmic transport (Lombet et al., 1985; Wonderlin and French, 1991) and incorporated into the axolemma by exocytotic vesicle fusion (Villegas and Villegas, 1981; Hammerschlag and Stone, 1982; Fried et al., 1991). The turnover cycle is presumably closed by internalization and reuse or degradation.

We propose that a shift in the local equilibrium of Na^+ channel insertion and internalization forms the basis for the remodeling of 7493 immunolabeling observed here. There are two main factors responsible for this shift: one *permissive* and one *promotional*. The principle permissive factor is the loss of myelin. In the presence of myelin, Na^+ channels are largely excluded from the subjacent axolemma. Demyelination, even when not accompanied by axotomy, permits their insertion (Waxman and Ritchie, 1985; England et al., 1990, 1991; Black et al., 1991). Contact with Schwann cell cytoplasm may be a key signal, as such contact is known to promote axolemmal Na^+ channel accumulation *in vitro* (Joe and Angelides, 1992, in press), while the presence of even a small number of insulating myelin lamellae appears to suppress it (Fig. 9*C*). The neuroglial signaling system cannot rely exclusively on Schwann cell contact, however, as Na^+ channels are excluded from paranodal membrane despite intimate contact with the Schwann cell cytoplasm in paranodal loops, and they are incorporated into axolemma under macrophages in the absence of close contact with Schwann cells.

While local demyelination and sprouting in neuromas *permits* ectopic insertion of Na^+ channels, a second factor may actively *promote* it. Specifically, in the normal economy of axons large numbers of Na^+ channels are transported centrifugally to subserve protein turnover at downstream nodes of Ranvier. This is particularly so for afferents, especially slowly adapting afferents, that have the extra burden of maintaining an Na^+ channel–rich impulse encoder at their sensory transducer ending (Katz, 1950; Quick et al., 1980; Seidel et al., 1990; Matzner and Devor, 1992). Following axotomy, many of these downstream targets no longer exist. As a result, in-transit channels are shunted into whatever membrane remains that is competent to receive them. The formerly internodal membrane at neuroma endings is a natural target, as it is both Na^+ channel impoverished and newly competent following myelin stripping. The combination of these two factors may account for the facts that neuromas are more hyperexcitable than patches of demyelination, and that sensory endings in neuromas are more hyperexcitable than motor endings (Devor, 1993).

Upstream from the neuroma, proximal nodes of Ranvier may also receive some of the now excess Na^+ channel protein, but probably not much as nodes are already close to saturation (Brismar et al., 1986). Finally, there may be extra Na^+ channel incorporation into the neurolemma at the level of the cell soma and, for motor neurons, on somatic dendrites. This could account for the hyperexcitability of these cells following axotomy (Wall and Devor, 1983; Burchiel, 1984; Titmus and Faber, 1990;

but see Gilly et al., 1990). It has yet to be determined whether Na^+ channel gene expression in the cell soma is upregulated (or downregulated) following axotomy (Sherman et al., 1985). However, proliferating Schwann cells at the injury site and distal to it release large quantities of NGF (Heumann et al., 1987), which is known to promote the upregulation of Na^+ channel expression on outgrowing neurites (Pollock et al., 1990).

Na^+ channel accumulation, and ectopic neural firing

We suggest that the appearance of 7493 immunoreactivity in formerly 7493-negative axolemma reflects the insertion of new functional voltage-sensitive Na^+ channels rather than, say, the marking of functional channels that were present previously but undetected, or the insertion of immunoreactive, but nonfunctional, channels. This assumption is supported by autoradiographic evidence for the accumulation of en-TTX binding sites in neuromas (Lombet et al., 1985), and electrophysiological evidence of elevated voltage-sensitive Na^+ conductance at cut axon ends and growth cones in invertebrate neurons (Belardetti et al., 1986; Gilly et al., 1990). Na^+ channels are an essential substrate of electrical excitability in peripheral nerve fibers (Hille, 1984). Moreover, we have shown using numerical simulation that increasing axolemmal Na^+ channel density, *without any other change in active or passive membrane properties*, can shift a neuron into a state of hyperresponsiveness to stimuli, and even from silence to a state of spontaneous repetitive discharge (Matzner and Devor, 1992). Thus, the observed accumulation of Na^+ channels at the end of transected nerves could, in itself, account for both the hyperexcitability of neuroma afferents, the resulting ectopic neural discharge and consequent neuropathic paresthesias and pain. Remodeling of other membrane associated channels and receptors, by the analogous process, could contribute to the anomalous mechano-, chemo-, and thermosensitivity associated with nerve injury sites (Devor, 1993).

References

Aitken JT, Thomas PK (1962) Retrograde changes in fiber size following nerve section. J Anat 96:121–129.

Angelides KJ, Loftus D, Elmer LW, Elson EL (1988) Distribution and lateral mobility of voltage-dependent sodium channels in neuronal cells. J Cell Biol 106:1911–1925.

Barres BA, Chun LLY, Corey DP (1990) Ion channels in vertebrate glia. Annu Rev Neurosci 13:441–474.

Belardetti F, Schacher S, Siegelbaum SA (1986) Action potentials, macroscopic and single channel currents recorded from growth cones of *Aplysia* neurones in culture. J Physiol (Lond) 374:289–313.

Bernstein JJ, Pagnanelli D (1982) Long-term axonal apposition in rat sciatic nerve neuroma. J Neurosurg 57:632–684.

Berthold C-H (1978) Morphology of normal peripheral axons. In: Physiology and pathobiology of axons (Waxman SG, ed), pp 3–63. New York: Raven.

Berthold C-H, Rydmark M (1983) Electron microscopic serial section analysis of nodes of Ranvier in lumbosacral spinal roots of the cat: ultrastructural organization of nodal compartments in fibers of different sizes. J Neurocytol 12:475–505.

Beuche W, Friede RL (1986) Myelin phagocytosis in Wallerian degeneration of peripheral nerve depends on silica-sensitive, bg/bg-negative and Fc-positive monocytes. Brain Res 378:97–106.

Black JA, Kocsis JD, Waxman SG (1990) Ion channel organization of the myelinated fibre. Trends Neurosci 13:48–54.

Black JA, Felts P, Smith KJ, Kocsis JD, Waxman SG(1991) Distribution of sodium channels in chronically demyelinated spinal cord axons: immuno-ultrastructural localization and electrophysiological observations. Brain Res 544:59-70.

Brismar T, Gilly WF (1987) Synthesis of sodium channels in the cell bodies of squid giant axons. Proc Natl Acad Sci USA 84:1459–1463.

Brismar T, Hildebrand C, Berglund S (1986) Nodes of Ranvier above a neuroma in the rat sciatic nerve: voltage clamp analysis and electron microscopy. Brain Res 378:347–356.

Burchiel KJ (1984) Spontaneous impulse generation in normal and denervated dorsal root ganglia: sensitivity to alpha-adrenergic stimulation and hypoxia. Exp Neurol 85:257–272.

Calvin W, Devor M, Howe J (1982) Can neuralgias arise from minor demyelination? Spontaneous firing, mechanosensitivity and afterdischarge from conducting axons. Exp Neurol 75:755–763.

Chan H, Smith RS, Snyder RE (1989) Junction between parent and daughter axons in regenerating myelinated nerve: properties of structure and rapid axonal transport. J Comp Neurol 283:391–404.

Chiu SY, Schwartz W (1987) Sodium and potassium currents in acutely demyelinated internodes of rabbit sciatic nerves. J Physiol (Lond) 391:631–649.

Devor M (1993) Pathophysiology of injured nerve. In: Textbook of pain, 3d ed (Wall PD, Melzack R, eds), in press. London, Wiley-Livingston.

Devor M, Bernstein JJ (1982) Abnormal impulse generation in neuromas: electrophysiology and ultrastructure. In: Abnormal nerves and muscles as impulse generators (Ochoa J, Culp W, eds), pp 363–380. Oxford: Oxford UP.

Devor M, Keller CH, Deerinck T, Levinson SR, Ellisman MH (1989) Na^+ channel accumulation on axolemma of afferents in nerve end neuromas in *Apteronotus*. Neurosci Lett 102:149–154.

Devor M, Keller CH, Ellisman MH (1990) Spontaneous discharge of afferents in a neuroma reflects original receptor tuning. Brain Res 517: 245–250.

Dodge FA, Cooley JW (1973) Action potential of the motoneuron. IBM J Res Dev 17:219–229.

Ellisman MH (1979) Molecular specializations of the axon membrane at nodes of Ranvier are not dependent upon myelination. J Neurocytol 8:719–735.

Ellisman MH, Levinson SR (1982) Immunocytochemical localization of sodium channel distributions in the excitable membranes of *Electrophorus electricus*. Proc Natl Acad Sci USA 79:6707–6711.

Ellisman MH, Miller JA, Agnew WS (1983) Molecular morphology of the tetrodotoxin-binding sodium channel protein from *Electrophorus electricus* in solubilized and reconstituted preparations. J Cell Biol 97:1834–1840.

Elmer LW, Black JA, Waxman SG, Angelides KJ (1990) The voltage-dependent sodium channel in mammalian CNS and PNS: antibody characterization and immunocytochemical localization. Brain Res 532:222–231.

England JD, Gamboni F, Levinson SR, Finger TF (1990) Changed distribution of sodium channels along demyelinated axons. Proc Natl Acad Sci USA 87:6777–6780.

England JD, Gamboni F, Levinson SR (1991) Increased numbers of sodium channels form along demyelinated axons. Brain Res 548:334–337.

Fried K, Govrin-Lippmann R, Rosenthal F, Ellisman MH, Devor M (1991) Ultrastructure of afferent axon endings in a neuroma. J Neurocytol 20:682–701.

Gilly WF, Lucero MT, Horrigan FT (1990) Control of the spatial distribution of sodium channels in giant fiber lobe neurons of the squid. Neuron 5:663–674.

Gray PTA, Ritchie JM (1985) Ion channels in Schwann and glial cells. Trends Neurosci 8:411–415.

Grissmer S (1986) Properties of potassium and sodium channels in frog internode. J Physiol (Lond) 381:119–134.

Haimovich B, Binilla E, Casadei J, Barchi R (1984) Immunolocalization of the mammalian voltage-dependent sodium channel using polyclonal antibodies against the purified protein. J Neurosci 4:2259–2268.

Hammerschlag R, Stone GC (1982) Membrane delivery by fast axoplasmic transport. Trends Neurosci 5:12–15.

Heumann R, Lindholm D, Bandtlow C, Meyer M, Radeke MJ, Misko TP, Shooter E, Thoenen H (1987) Differential regulation of mRNA encoding nerve growth factor and its receptor in rat sciatic nerve during development, degeneration and regeneration: role of macrophages. Proc Natl Acad Sci USA 84:8735–8739.

Hildebrand C (1989) Myelin sheath remodelling in remyelinated rat sciatic nerve. J Neurocytol 18:285–294.

Hildebrand C, Mustafa GY, Waxman SG (1986) Remodelling of internodes in regenerated rat sciatic nerve: electron microscopic observations. J Neurocytol 15:681–692.

Hille B (1984) Ionic channels of excitable membranes, pp 1–426. Sunderland, MA: Sinauer.

Joe E-H, Angelides KJ (1992) Clustering of voltage-dependent sodium channels on axons depends on Schwann cell contact. Nature 356:333–335.

Joe E-H, Angelides KJ (in press) Clustering and mobility of voltage-dependent sodium channels during myelination, in press.

Johnson RD, Munson JB (1991) Regenerating sprouts of axotomized cat muscle afferents express characteristic firing patterns to mechanical stimulation. J Neurophysiol 66:2155–2158.

Katz B (1950) Depolarization of sensory terminals and the initiation of impulses in the muscle spindle. J Physiol (Lond) 111:261–282.

Kordel E, Davis J, Trapp BD, Bennett V (1990) An isoform of ankyrin is localized at nodes of Ranvier in myelinated axons of central and peripheral nerves. J Cell Biol 110:1341–1352.

Koschorke GM, Mayer RA, Tillman DB, Campbell JN (1991) Ectopic excitability of injured nerves in monkey: entrained responses to vibratory stimuli. J Neurophysiol 65:693–701.

Lombet A, Laduron P, Mourre C, Jacomet Y, Lazdunski M (1985) Axonal transport of the voltage-dependent Na^+ channel protein identified by its tetrodotoxin binding site in rat sciatic nerves. Brain Res 345:153–158.

Mackenzie ML, Shorer Z, Ghabriel MN, Allt G (1984) Myelinated nerve fibers and the fate of lanthanum tracer: an *in vivo* study. J Anat 138:1–14.

Matsumoto E, Rosenbluth, J (1985) Plasma membrane structure at the axon hillock, initial segment and cell body of frog dorsal root ganglion cells. J Neurocytol 14:731–747.

Matzner O, Devor M (1992) Na^+ conductance and the threshold for repetitive neuronal firing. Brain Res 597:92–98.

Morris JH, Hudson AR, Weddell G (1972) A study of degeneration and regeneration in the divided rat sciatic nerve based on electron microscopy, I–IV. Z Zellforsch Mikrosk Anat 124:76–203.

Nordin M, Nystrom B, Wallin U, Hagbarth K-E (1984) Ectopic sensory discharges and paresthesiae in patients with disorders of peripheral nerves, dorsal roots and dorsal columns. Pain 20:231– 245.

Nystrom B, Hagbarth KE (1981) Microelectrode recordings from transected nerves in amputees with phantom limb pain. Neurosci Lett 27:211–216.

Ochoa J, Torebjork HE, Culp WL, Schady W (1982) Abnormal spontaneous activity in single sensory nerve fibers in humans. Muscle Nerve 5:574–577.

Papir-Kricheli D, Devor M (1988) Abnormal impulse discharge in primary afferent axons injured in the peripheral and central nervous system. Somatosens Mot Res 6:63–77.

Pappone PA, Cahalan MD (1985) Demyelination as a test for a mobile Na channel modulator in frog node of Ranvier. Biophys J 47:217–223.

Pfenninger KH (1982) Transport and insertion of membrane components into processes of growing neurons. Neurosci Res Prog Bull 20:73–79.

Pollock JD, Krempin M, Rudy B (1990) Differential effects of NGF, FGF, EGF, cAMP and dexamethasone on neurite outgrowth and sodium channel expression in PC12 cells. J Neurosci 10:2626–2637.

Quick W, Kennedy WR, Poppele RE (1980) Anatomical evidence for multiple sources of action potentials in the afferent fibers of muscle spindles. Neuroscience 5:109–115.

Revel JM, Karnovsky MJ (1967) Hexagonal array of subunits in intercellular junctions of the mouse heart and liver. J Cell Biol 33:C7–C12.

Ritchie JM, Black JA, Waxman SG, Angelides KJ (1990) Sodium channels in the cytoplasm of Schwann cells. Proc Natl Acad Sci USA 87:9290–9294.

Rosenbluth J (1983) Intramembranous particle distribution in nerve fiber membranes. Experientia 39:953–963.

Ruiz JA, Kocsis JD, Preson RJ (1981) Repetitive firing characteristics of mammalian myelinated axons: an intra-axonal analysis. Soc Neurosci Abstr 7:904.

Schmidt JW, Caterrall WA (1986) Biosynthesis and processing of the α subunit of the voltage-sensitive sodium channel in rat brain neurons. Cell 46:437–445.

Seidel WM, Popper AN, Chang JS (1990) Spatial and morphological differentiation of trigger zones in afferent fibers to the teleost utricle. J Comp Neurol 302:629–642.

Sherman SJ, Chrivia J, Catterall WA (1985) Cyclic adenosine 3′:5′-monophosphate and cytosolic calcium exert opposing effects on biosynthesis of tetrodotoxin-sensitive sodium channels in rat muscle cells. J Neurosci 5:1570–1576.

Small RK, Blank M, Ghez R, Pfenninger KH (1984) Components of the plasma membrane of growing axons. II. Diffusion of membrane protein complexes. J Cell Biol 98:1434–1443.

Srinivasan Y, Elmer LW, Davis JQ, Bennett V, Angelides KJ (1988) Ankyrin and spectrin associates with voltage-dependent sodium channels in brain. Nature 333:177–180.

Strichartz GR, Small RS, Pfenninger KH (1984) Components of the plasma membrane of growing axons. III. Saxitoxin binding to sodium channels. J Cell Biol 98:1444–1452.

Titmus MJ, Faber DS (1990) Axotomy-induced alterations in the electrophysiological characteristics of neurons. Prog Neurobiol 35:1–51.

Vahle-Hinz C, Gottschaldt K-M, Kraft H (1987) Morphological basis for 'ephaptic' excitation in neuroma nerves. In: Effects of nerve injury on trigeminal and spinal somatosensory systems (Pubols LM, Sessle BJ, eds), p 487. New York: Liss.

Villegas R, Villegas GM (1981) Nerve sodium channel incorporation in vesicles. Annu Rev Biophys Bioeng 10:387–419.

Wall PD, Devor M (1983) Sensory afferent impulses originate from dorsal root ganglia as well as from the periphery in normal and nerve-injured rats. Pain 17:321–339.

Waxman SG, Quick DC (1978) Functional architecture of the initial segment. In: Physiology and pathobiology of axons (Waxman SG, ed), pp 125–130. New York: Raven.

Waxman SG, Ritchie JM (1985) Organization of ion channels in the myelinated nerve fiber. Science 228:1502–1507.

Wollner DA, Catterall WA (1986) Localization of sodium channels in axon hillocks and initial segments of retinal ganglion cells. Proc Natl Acad Sci USA 83:8424–8428.

Wonderlin WF, French RJ (1991) Ion channels in transit: voltage-gated channels in axoplasmic organelles of the squid *Loligo pealei*. Proc Natl Acad Sci USA 88:4391–4395.

Zelena J, Lubinska L, Gutman E (1968) Accumulation of organelles at the end of interrupted axons. Z Zellforsch Mikrosk Anat 91:200–219.